Area-Specific Seismic Noise Reference Curves in an Urban Volcanic Environment: The Campi Flegrei Case

Roberta Esposito *, Lucia Nardone, Roberto Manzo, Guido Gaudiosi, Massimo Orazi

Posted Date: 5 May 2026

doi: 10.20944/preprints202605.0239.v1

Keywords: ambient seismic noise; power spectral density; Campi Flegrei caldera

 doi:10.20944/preprints202605.0239.v1

Article

Area-Specific Seismic Noise Reference Curves in an Urban Volcanic Environment: The Campi Flegrei Case

Roberta Esposito *, Lucia Nardone, Roberto Manzo, Guido Gaudiosi and Massimo Orazi

Istituto Nazionale di Geofisica e Vulcanologia, Sezione di Napoli, Osservatorio Vesuviano

* Correspondence: roberta.esposito@ingv.it

Abstract

The study investigates the seismic ambient noise within the Campi Flegrei caldera (Naples, Italy) to improve the detection capability and reliability of the local earthquake monitoring system managed by the INGV, Osservatorio Vesuviano. It focuses on the spectral characteristics and spatial variability of the ambient noise field, aiming to identify the dominant frequency bands that control signal detectability and to provide key information for the optimization of the monitoring network. Due to the dense urban environment surrounding the caldera, seismic recordings are often contaminated by high anthropogenic noise, which can mask low-magnitude volcanic or seismic signals. Power Spectral Density (PSD) analysis was applied to evaluate background noise levels at several broadband stations belonging to both the permanent and temporary seismic networks over the period January 2022 to January 2023. The resulting PSD estimates were compared with the global Peterson noise models to assess station performance and environmental conditions. Results show significant variability among stations, related to local human activity, proximity to infrastructure and different installation settings (buried vs. surface). The study emphasizes the importance of continuous noise monitoring to ensure high-quality seismic data, support optimal station siting, and refine monitoring strategies in densely populated volcanic regions such as Campi Flegrei, where the reliable detection of low-amplitude seismic and volcanic signals is essential.

Keywords: ambient seismic noise; power spectral density; Campi Flegrei caldera

1. Introduction

The Campi Flegrei caldera, located in Pozzuoli near the city of Naples in southern Italy, is one of the most active and complex volcanic systems in Europe (REF). Its dense urban setting, combined with ongoing ground deformation, hydrothermal activity, and frequent low-magnitude seismicity, presents major challenges for seismic monitoring. In this environment, background seismic noise generated by traffic, industrial activity, urban vibrations, ocean microseisms, wind and hydrothermal circulation can significantly elevate noise levels [1]. As a result, low-amplitude signals related to volcano-tectonic activity or fluid migration could be obscured, reducing the reliability and precision of the monitoring system. As an example we show in Figure 1 a low-magnitude (Md=1.1, Date: 23/12/2024, Time: 10:24:52 UTC) event from the seismic catalog of Campi Flegrei [2] recorded within the caldera at a depth of 1.9 Km. The waveforms highlight how small-amplitude seismic signals are embedded within a noisy urban environment, despite the very short hypocentral distances between the events and the stations shown in the figure, illustrating the challenges in distinguishing volcanic microseismicity from background noise.

Evaluating the spatial and temporal variability of background seismic noise in the Campi Flegrei caldera is therefore essential for enhancing the fidelity of seismic signals and improving network performance. A robust characterization of ambient noise helps distinguish between natural and human-induced sources, identifies stations or time periods with reduced data quality and guides the

 doi:10.20944/preprints202605.0239.v1

application of optimal filtering strategies. It also provides critical insights for refining the configuration of the seismic network, including station placement and sensor upgrades. Overall, seismic noise assessment is key to optimizing station performance and ensuring reliable real-time monitoring of the volcanic and tectonic processes. High-quality seismic data are fundamental for multiple applications, including earthquake localization, source parameter analysis, seismic tomography, and monitoring temporal variations in seismic velocity, which require a low noise floor to ensure precision and completeness [3,4]. Urban stations are particularly affected by high-frequency noise within the 0.1–1 s period band, which is critical for detecting both body and surface waves. This makes the Campi Flegrei caldera the most challenging volcanic environment for seismic monitoring in Italy. Background noise in the area originates from both anthropogenic sources (e.g., traffic, industrial operations, urban activities) and natural processes (e.g., oceanic microseisms, atmospheric pressure variations, wind-induced vibrations) [5–7].

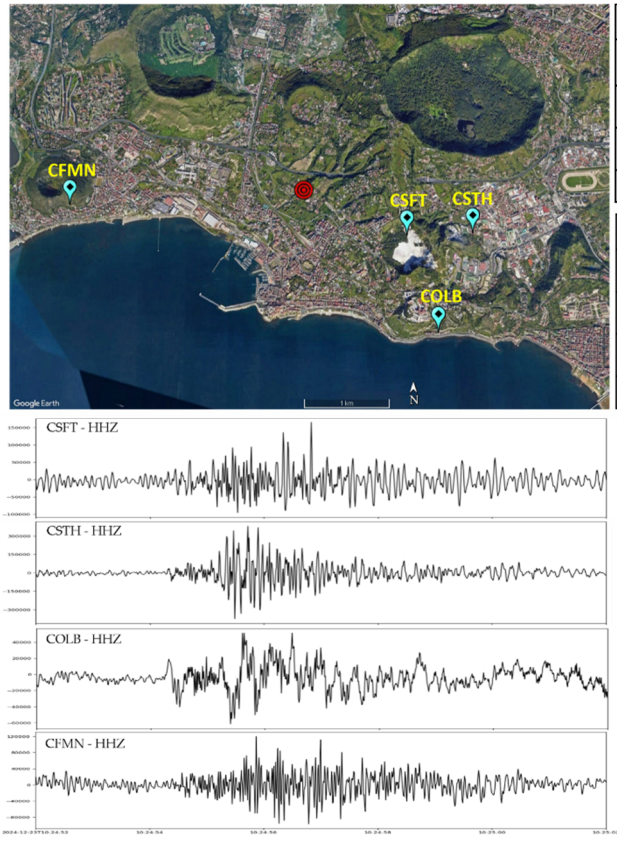

Seismic event information	
Date Time	23/12/2024 10:24:52 UTC
Latitude	40N 50.04
Longitude	14° 07.49
Depth	1.9 Km

Station	Epicentral distance
CSFT	1.3 Km
CSTH	2.3 Km
COLB	2.6 Km
CFMN	2.8 Km

Figure 1. Location of a M 1.1 (Date: 23/12/2024, Time: 10:24:52 UTC) earthquake within the Campi Flegrei caldera (red circle) and corresponding vertical-component waveforms recorded at selected seismic stations (CSFT, CSTH, COLB, CFMN).

To quantitatively evaluate noise conditions, this study employs Power Spectral Density (PSD) analysis as the main analytical tool. PSD represents how seismic energy is distributed over frequency, providing detailed insights into station performance, environmental conditions and the influence of external sources. This frequency-dependent assessment allows evaluation of how different wavelengths are affected by local site effects, installation depth and surrounding activities. The observed PSD curves are compared against the global noise reference models proposed by Peterson (1993) [8], namely the New Low Noise Model (NLNM) and the New High Noise Model (NHNM), widely used as benchmarks for assessing seismic station quality. The comparison allows us to identify deviations associated with local environmental conditions or site-specific characteristics. In the Campi Flegrei area, seismic stations experience markedly different noise levels depending on their installation type—surface vs. borehole—and proximity to urbanized zones or industrial

 doi:10.20944/preprints202605.0239.v1

infrastructures. Underground installations typically show reduced noise levels (up to ~20 dB lower) due to isolation from surface disturbances, while surface stations are more exposed to anthropogenic and meteorological noise.

The data collected by the Permanent and Mobile Seismic Networks of the INGV,Osservatorio Vesuviano [9,10], spanning from January 2022 to January 2023, provide a comprehensive basis for evaluating spatial and temporal variability across the caldera. The networks covers areas ranging from coastal zones—where microseismic noise generated by ocean waves is predominant—to inland and heavily urbanized regions dominated by anthropogenic noise [11]. The influence of sea-wave activity is particularly evident in the 1–10s period range, where the secondary microseism peak shifts relative to the Peterson reference curves, consistent with observations in coastal environments [12].

Furthermore, the analysis highlights how local environmental and infrastructural conditions can alter PSD amplitude. For example, stations installed in proximity of railways, although in shielded environments such as tunnels, may still exhibit strong low-frequency noise due to train traffic, with amplitude variations exceeding 40 dB compared to reference models during daytime hours. Conversely, surface stations located in densely urbanized zones show persistently high PSD amplitudes across all components, especially for frequencies below 0.3 s, where anthropogenic activity dominates.

2. Materials and Methods

The analysis was carried out using data acquired by the Permanent and Mobile Seismic Networks operated by the Istituto Nazionale di Geofisica e Vulcanologia (INGV) – Osservatorio Vesuviano, which monitor the Campi Flegrei caldera through a dense distribution of broadband seismic stations. The dataset covers the period from January 2022 to January 2023 for most of the stations, although shorter time spans were considered for those with intermittent data availability. The seismic networks include both surface and borehole installations, distributed across areas characterized by different environmental and anthropogenic conditions. In Table 1, the specifications of each station are reported, including the type of installed sensor and digitizer. These networks play a crucial role in the continuous surveillance of the caldera and have been progressively upgraded to improve data quality and resilience, particularly in areas with high background noise and complex site conditions [13], also in response to the ongoing unrest.

Table 1. Technical specifications of the seismic stations considered in this study.

Station name	Sensor			Digitizer	
	Manufacturer	Model	Low Freq. Corner period (s)	Manufacturer	Model
ACL2	Lennartz	LE3D	20	Nanometrics	Taurus
ASBG	Guralp	40T	60	Lennartz	Marslite
CAAM	Guralp	3ESPC	120	Guralp	Affinity
CBAC	Guralp	3T	120	Guralp	Affinity
CFMN	Guralp	3ESPC	120	Guralp	Affinity
CMIS	Guralp	3ESPC	120	INGV	Gilda
CMSA	Guralp	40T	60	INGV	Gilda
CNIS	Guralp	3ESPC	120	Guralp	Affinity
COLB	Guralp	3ESPC	120	Guralp	Affinity
CPIS	Guralp	40T	60	INGV	Gilda
CPOZ	Guralp	40T	120	INGV	Gilda
CROS	Guralp	40T	60	Lunitek	Atlas C

 doi:10.20944/preprints202605.0239.v1

CSFT	Guralp	40T	60	INGV	Gilda
CSOB	Guralp	3ESPC	120	Guralp	Affinity
CSTH	Guralp	3ESPC	120	Guralp	Affinity
MIRG	Guralp	40T	60	Lennartz	Marslite
OVDG	Geotech	KS2000	120	Lennartz	Marslite
PCNG	Guralp	40T	60	Nanometrics	Taurus
PESG	Guralp	40T	60	Lennartz	Marslite
PNB2	Lennartz	LE3D	20	Lennartz	Marslite
RENG	Guralp	40T	60	Lennartz	Marslite
UMBG	Geotech	KS2000	120	Reftek	RT130
UMSG	Geotech	KS2000	120	Reftek	RT130
VIRG	Guralp	40T	60	Reftek	RT130

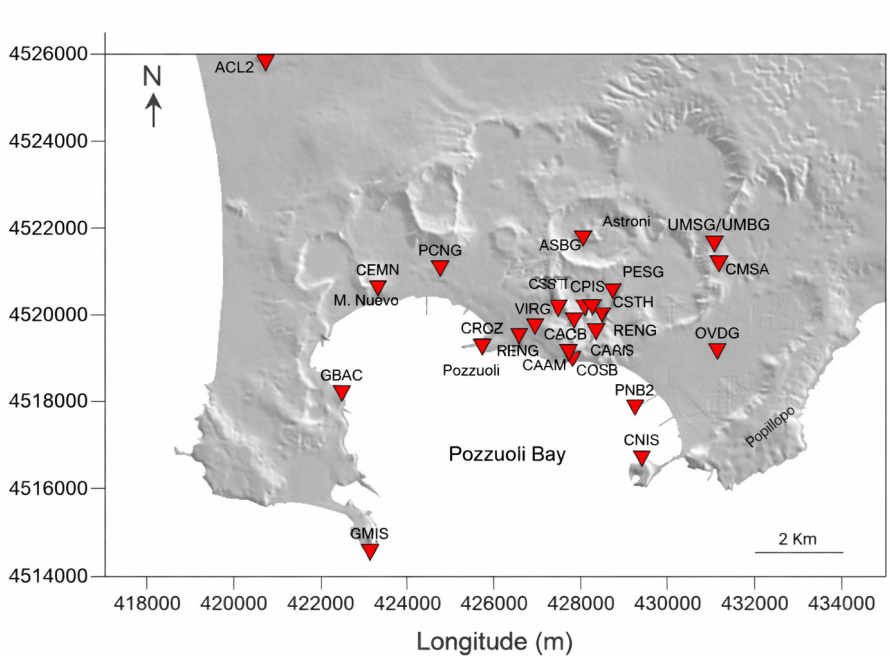

Figure 2. Map of Campi Flegrei. Red triangles represent seismic stations of permanent and mobile networks of INGV - Osservatorio Vesuviano used in this study. Station UMBG (borehole installation) coincides with the location of UMSG on the map.

Continuous three-component seismic data (Z, N, E) were processed to evaluate the ambient seismic noise at each site. A series of preprocessing steps were applied to ensure data quality, following standard procedures adopted in noise analysis and network monitoring studies [14].

Visual and automated checks were performed to remove time segments affected by instrumental errors, telemetry issues or transient seismic events (local or teleseismic earthquakes). The cleaned continuous recordings were then divided into 3600-second non-overlapping windows, which form the basis for the spectral analysis [15].

The noise level at each seismic station was evaluated using the Power Spectral Density (PSD), which quantifies how seismic signal energy is distributed as a function of frequency. Each 1-hour window was detrended, tapered (using a cosine taper), and transformed into the frequency domain through a Fast Fourier Transform (FFT).

$$X(f) = \int_{-\infty}^{\infty} x(t)\, e^{-i2\pi ft} dt,$$

 doi:10.20944/preprints202605.0239.v1

where T is the window length and f denotes frequency. The PSD for each window was estimated as the squared modulus of the Fourier spectrum, properly normalized by the window length and the tapering function:

$$PSD(f) = \frac{2}{T}|X(f)|^2,$$

where T is the duration of the analyzed time window, and the factor 2 accounts for the one-sided spectrum. Instrument response was removed to express PSD values in physical units of ground acceleration. For consistency with standard ambient noise studies, PSD values were converted to decibels (dB) according to

$$PSD_{dB}(f) = 10log_{10}\big(PSD(f)\big).$$

Given the strong temporal variability of seismic noise in densely urbanized environments, individual PSD estimates were not averaged into a single representative spectrum. Instead, the results are presented using the Probabilistic Power Spectral Density (PPSD) approach [16], which provides a statistical characterization of noise levels over time. The PPSD is constructed by stacking all PSDs computed from the hourly windows and sorting them into amplitude bins for each frequency (or period). For a given frequency f, the PPSD represents the probability density function $P\,(A/f)$ of observing a spectral amplitude A:

$$P(A|f) = \frac{N\,(A,f)}{N_{tot}(f)},$$

where $N\,(A/f)$ is the number of PSD estimates falling within a given amplitude bin and $N_{tot}\,(f)$ is the total number of PSD estimates at that frequency.

The resulting PPSD distributions are displayed as color-coded histograms in the period–amplitude domain, where color intensity indicates the percentage of time during which a given noise level is observed. This representation allows identification of both typical noise conditions (e.g., median or modal values) and extreme noise levels associated with specific environmental or anthropogenic sources. The observed PPSD curves were compared with the global New Low Noise Model (NLNM) and New High Noise Model (NHNM) proposed by Peterson.

An example of the computed PPSDs for stations of the Campi Flegrei network is shown in Figure 3. Each plot displays the probability distribution of PPSD values as a function of period (horizontal axis, in seconds) and spectral amplitude (vertical axis, in decibels). The color scale shown on the right represents the percentage of time during which a specific PSD amplitude occurs at each frequency. Warmer colors (magenta to red) indicate the most frequently observed noise levels, while cooler colors represent less frequent amplitudes.

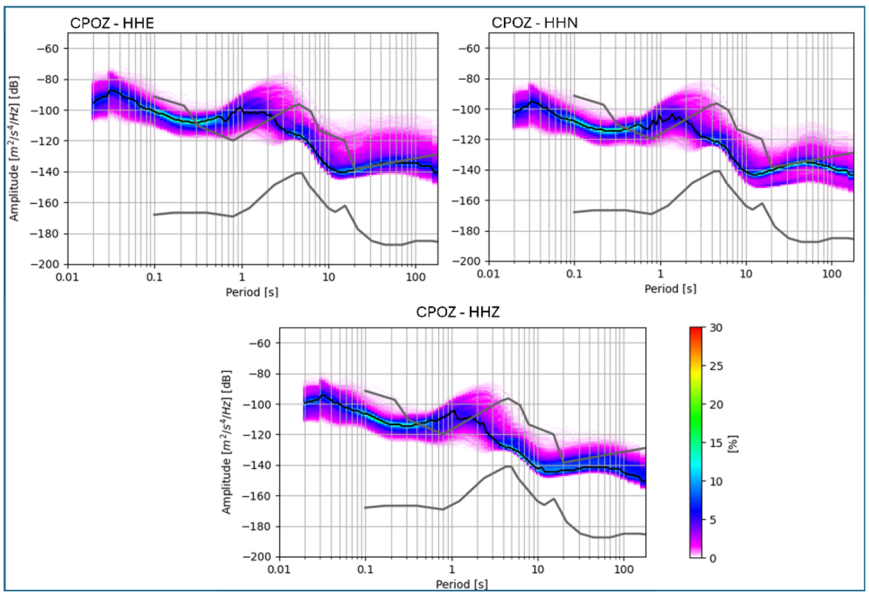

 doi:10.20944/preprints202605.0239.v1

Figure 3. PPSD curves for horizontal and vertical components of CPOZ station. Grey curves represent the New High Noise Model and New Low Noise Model, respectively, while the black curves are the average curves of the PPSD distributions.

This graphical representation highlights how the ambient noise varies over time and for any frequency. For instance, higher amplitudes in the 0.01–1 s period band correspond to persistent anthropogenic noise, while the broad peak around 1–10 s represents the secondary microseism, typically generated by ocean wave interactions along the coastline. Secondary microseisms are generated by nonlinear interaction of ocean waves and may be strongly modulated by coastal morphology [17]. The reduction in spectral amplitude at longer periods (>10 s) reflects the dominance of natural, low-frequency background motion with sources related to atmospheric pressure fluctuations, wind effects or thermoelastic ground effects.

3. Results

3.1. Time Variation of Seismic Noise and the Influence of Installation Conditions

Figure 4 illustrates the probabilistic power spectral density (PPSD) distributions for the COLB seismic stations under different traffic conditions of the Cumana railway, which runs beneath the tunnel hosting the site. The three panels on the left show the PPSDs calculated over the entire analysis period (January 2022 – January 2023), corresponding to regular railway operation and highlighting the ambient seismic noise levels associated with routine train traffic. The influence of passing trains is clearly visible, particularly at long periods (> 5 s), where spectral amplitudes increase significantly. In contrast, the panels on the right refer to a one-month interval (January 2026) during which train traffic was completely suspended, allowing an evaluation of the station's baseline noise level in the absence of railway-induced vibrations.

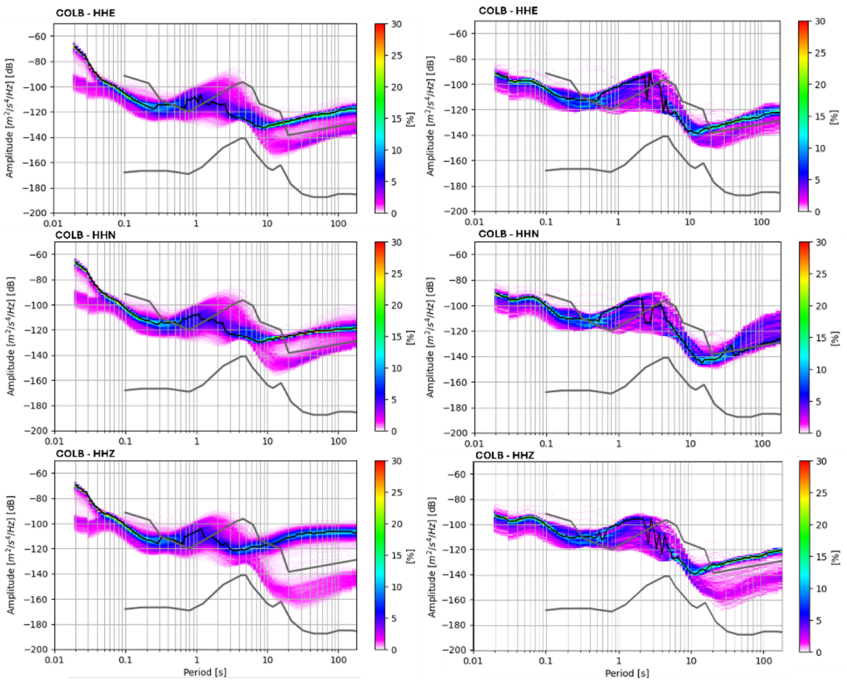

Figure 4. PPSD curves for horizontal and vertical components of COLB station. On the left PPSDs for station COLB computed from January 2022 to January 2023, on the right PPSDs during suspension of Cumana railway traffic.

A comparable behavior has been previously observed in the Campi Flegrei area at the nearby BGNG seismic station, whose power spectral density was analyzed by La Rocca and Galluzzo 2015 [1] using one month of continuous data. Their results highlighted the presence of significant

 doi:10.20944/preprints202605.0239.v1

anthropogenic noise contributions, particularly at very low frequencies, associated with the passage of trains running close to the station. In that case, as well, the PSD displayed two distinct branches at frequencies lower than about 0.1 Hz (in Figure 4 higher that 10s), corresponding respectively to nighttime conditions and daytime recordings strongly affected by train traffic.

Figure 5 shows the Probabilistic Power Spectral Densities (PPSD) of the vertical (HHZ) components for stations UMSG and UMBG, both part of the mobile seismic network at the Monte Sant'Angelo University campus. Although installed at the same location, UMSG is located at the surface while UMBG is installed underground in a borehole at a depth of 144m.

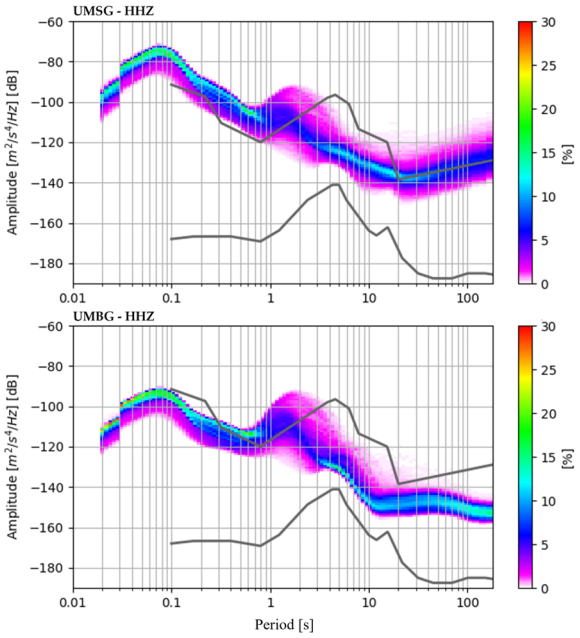

Figure 5. Comparison of PPSD curves for the vertical (HHZ) components of stations UMSG (surface) and UMBG (underground).

The plots highlight the effect of installation depth on ambient seismic noise. The surface station (UMSG) exhibits higher amplitudes at high frequencies (<1 Hz), reflecting environmental and anthropogenic noise such as traffic, wind, and human activity. In contrast, the underground station (UMBG) (consistent with results of [3,18,19]) shows significantly lower noise levels, with reductions of approximately 20–40 dB in the low-frequency range, depending on the frequency band.

Additionally, the PPSD curves of the borehole station are smoother and less scattered, indicating more stable and less variable seismic signals. The noise reduction is also observed at higher frequencies (>10 Hz), where the underground installation further suppresses short-period vibrations likely caused by local surface disturbances. This comparison clearly demonstrates the advantage of underground installation in mitigating both low- and high-frequency surface noise, improving the overall quality of seismic observations.

The plots in Figure 6 show the probabilistic power spectral densities (PPSD) of the CBAC and CFMN stations. The CBAC station is installed inside an ancient Roman cistern dug into the tuff beneath the Baia Castle and, despite being located in a highly urbanized environment, the deep installation exhibits good noise performance. A comparison with the CFMN station reveals a systematic reduction in seismic noise at CBAC, particularly at periods shorter than 1 s and longer than 10 s, where noise levels are reduced by at least ~10 dB. At short periods (T < ~0.3 s), anthropogenic noise is strongly attenuated by the site of installation, with amplitude levels consistently falling below the Peterson New High Noise Model (NHNM) by approximately 5–15 dB across all three components. At intermediate periods (T ≈ 1–10 s), noise levels remain relatively stable and comparable among the components, with median amplitudes generally lying between the Peterson New Low Noise Model (NLNM) and NHNM curves. Overall, these observations indicate

 doi:10.20944/preprints202605.0239.v1

that the deep installation efficiently suppresses surface-related noise sources and provides a low-noise recording environment over a broad period range.

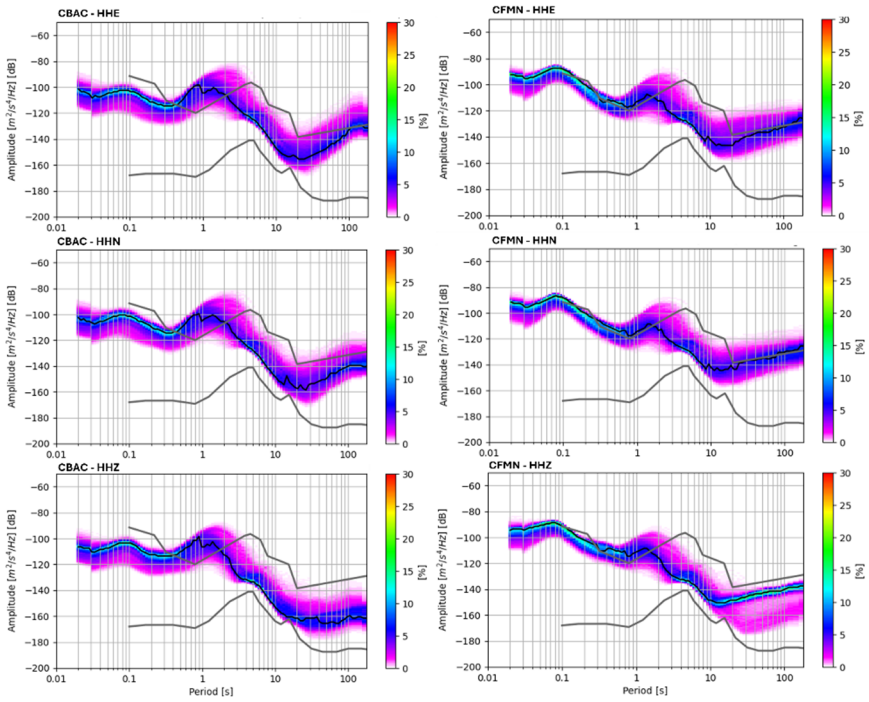

Figure 6. PPSD curves for horizontal and vertical components of station CBAC and CFMN. Grey curves represent the New High Noise Model and New Low Noise Model, respectively, while the black curves are the average curves of the PPSD distributions.

The CFMN station, even with careful sensor installation, is located on the surface within a highly urbanized area. In the period below 0.3 seconds, the impact of anthropogenic activity is clear across all three components. The PSD amplitude values consistently reach or exceed the reference NHNM curves throughout the analyzed period.

In the period range 0.4-10 seconds, both stations exhibit a peak (known as Secondary Microseismic Noise Peak) that is shifted relative to the maximum in the reference curves. This behavior, already noted by Vassallo et al. [6], is clearly observed across all the stations analyzed in this study. The ambient noise level in the seismic spectrum in this period band is strongly influenced by the geographic location of the seismic station, particularly by the proximity to the coastline, as well as by the general effect of seasonal variation.

It has been observed that the peak of secondary microseisms occurs at shorter periods ($T \approx 2$ s) in shallow inland seas compared to oceans ([20] and reference therein). This phenomenon is also strongly influenced by coastal morphology, which can promote internal resonances along bays or fjords [21]. In the Campi Flegrei caldera the Pozzuoli bay provides a typical example: a shallow inland sea, open between Nisida and Miseno and widening inland (see Figure 2). Our PPSD analysis shows a systematic shift of the secondary microseism peak toward shorter periods compared to reference values, highlighting distinctive “spectral fingerprints” associated with the coastal morphology and its influence on microseism generation and spectral characteristics.

3.2. Site Control on Seismic Noise Amplitudes

Figure 7 shows the Solfatara-Pisciarelli area within the Campi Flegrei caldera, highlighting the locations of three selected seismic stations analyzed in this study, all within a radius of approximately 800 m. Although in close proximity, the stations are installed in significantly different geological, morphological, and topographical settings: CSFT inside the Solfatara crater, in close proximity to the

 doi:10.20944/preprints202605.0239.v1

main fumarolic vents, CSOB at the far end of the eastern rim of the crater, and CSTH in the Agnano Plain, a morphologically flatter sector of the caldera.

Figure 7. Map of Pozzuoli area where the stations CSFT, CSOB and CSTH are located.

Figure 8 presents the probabilistic power spectral density (PPSD) estimates for the three Campi Flegrei stations—CSOB, CSFT, and CSTH—highlighting clear differences in noise characteristics across the frequency spectrum, closely linked to their geological, morphological, and environmental settings. CSTH, the long-established reference station for the area, consistently exhibits the lowest and most stable noise levels, with narrow distributions that closely follow global low-noise models, especially in the mid- and high-frequency ranges. CSOB, located on the upper flank of the Solfatara crater, shows moderately higher noise, particularly in the mid-frequency band between ~0.1 and 1 s, where topographic exposure and local site amplification effects contribute to a broader distribution [22,23]. The most distinctive behavior is observed at CSFT seismic station, located inside the Solfatara crater and closest to the area with an intense fumarolic activity [24]. The latter displays a pronounced increase in high-frequency noise (<0.2 s), where the persistent degassing and turbulent flow of the fumarole produce elevated and highly variable spectral levels. This locally generated energy could be further amplified by the presence, within the crater, of highly heterogeneous, strongly altered (e.g., thermally) and stratified volcanic deposits. Petrosino et al. (2012) studying the structure of the Solfatara crater and using H/V spectral ratios, highlighted that in the 0.1–1 s period band there is a marked amplification, which could be responsible for further enhancing the spectral energy associated with the fumarolic activity.

At longer periods (> 10 s), all stations show a gradual rise in noise typical of microseismic sources.

3.3. Spatial Variations of Seismic Noise

Due to the dense coverage of the seismic network, we analyzed the spatial distribution of PPSD amplitudes at four reference periods (0.07 s, 0.1 s, 1.3 s and 10 s in Figure 9), chosen according to the patterns highlighted in the previous results.

The spatial distribution of PPSD amplitudes across the Campi Flegrei area is shown in Figure 9. It was obtained using the SciPy library (scipy.interpolate.griddata) with cubic interpolation, which creates a smooth and continuous curve that passes exactly through a set of known data points. It reveals clear frequency-dependent patterns of seismic noise, highlighting the influence of local site effects and variations in noise sources. The maps illustrate how short-, intermediate-, and long-period components of seismic noise are differently distributed across the region, reflecting the combined impact of surface conditions, anthropogenic activity, and environmental processes.

 doi:10.20944/preprints202605.0239.v1

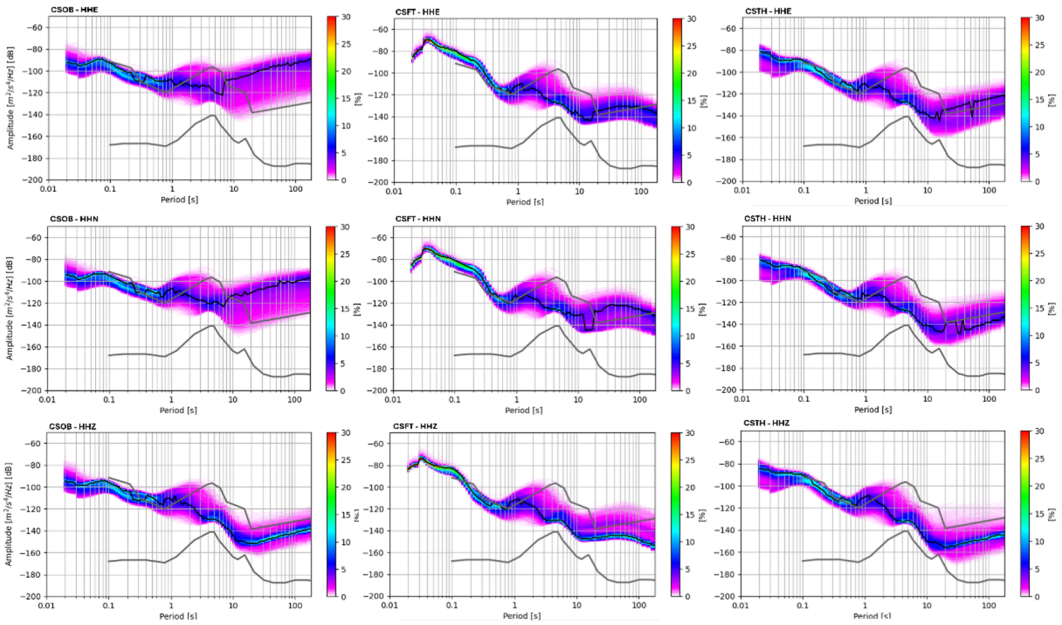

Figure 8. PPSD curves for horizontal and vertical components of CSOB, CSFT and CSTH stations. Grey and black curves represent respectively Peterson curves (New High Noise Model and New Low Noise Model) and the average curves of the PPSD distributions.

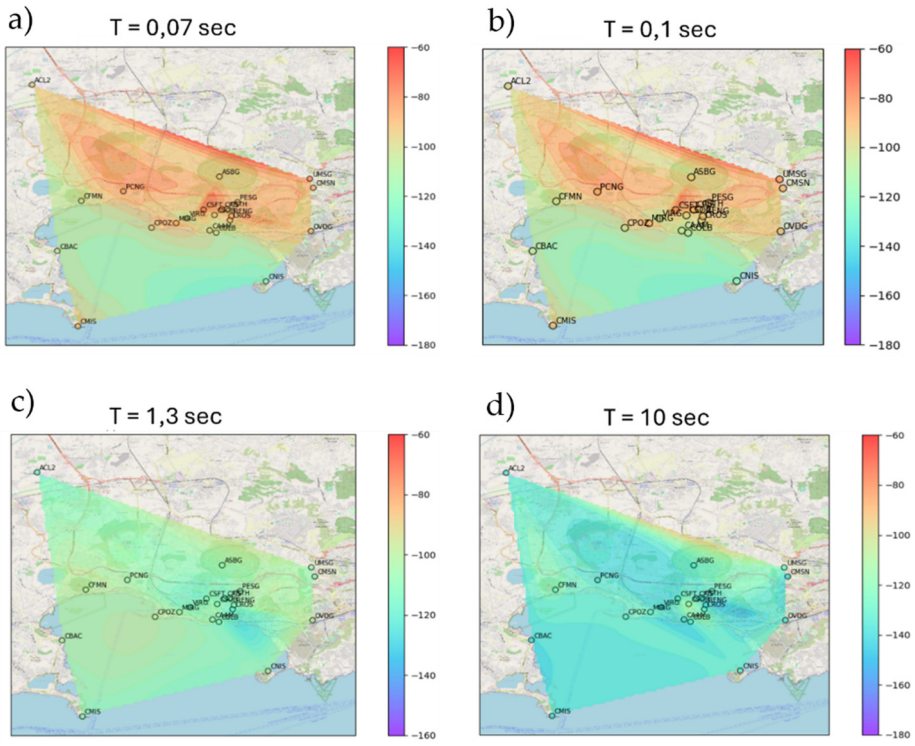

Figure 9. Spatial distribution of PPSDs amplitudes in the area of Campi Flegrei. a) PPSDs at 0.07s; b) PPSDs at 0.1 s; c) PPSDs at 1.3s and d) PPSD at 10s.

At the shortest periods (0.07 s and 0.1 s), the PPSD amplitude maps show a pronounced concentration of high energy in the central and northern sectors, forming a triangular region of elevated spectral levels that coincides with the most active portion of the caldera. These high-frequency amplitudes are strongly influenced by shallow geological conditions and amplified by pervasive anthropogenic noise, which is abundant in the densely urbanized areas surrounding

 doi:10.20944/preprints202605.0239.v1

Pozzuoli and the Solfatara crater. In a volcanically active and structurally complex area such as Campi Flegrei, high-frequency seismic noise is expected to be particularly sensitive to shallow heterogeneities, including altered volcanic deposits and strong lateral velocity contrasts. Previous array-based and tomographic studies demonstrate that these conditions can generate pronounced spatial variations in noise amplitudes at short periods [23,25–27]. In addition to local site effects and hydrothermal activity, human-induced vibrations—traffic, industrial activity, and urban infrastructure—contribute substantially to the observed increase in short-period energy [1]. Conversely, the southern coastal sector consistently exhibits lower PSD amplitudes, indicating more efficient attenuation of high-frequency noise and reduced exposure to anthropogenic sources.

At 1.3 s, the energy distribution becomes more diffuse, and the influence of regional microseisms becomes apparent. Enhanced PPSD levels over the coastline and adjacent marine areas indicate the contribution of ocean-generated waves that propagate inland. This intermediate period marks a transition from strong local, high-frequency effects—both natural and anthropogenic—to processes governed by regional environmental sources. The spatial pattern at this period shows reduced contrast between high- and low-energy areas, reflecting the longer wavelengths and diminished scattering associated with microseismic generation.

In Figure 9d (10s), the PPSD amplitudes become increasingly homogeneous across the caldera. Both coastal and inland regions show nearly uniform energy levels, underscoring the fact that long-period noise components penetrate deeper into the crust and are largely unaffected by surface-level heterogeneities or human activity. The absence of pronounced localized anomalies at this period highlights the dominance of deeper structural controls on the ambient seismic field. Overall, the frequency-dependent PPSD maps reveal how seismic noise propagates and attenuates within the caldera.

4. Discussion

The main objective of this study was to evaluate the ambient seismic noise conditions across the Campi Flegrei caldera and to assess how local environmental, geological, and anthropogenic factors [28] influence the performance of the seismic monitoring network. The results demonstrate that noise levels are highly heterogeneous in both space and frequency, confirming that background seismic noise represents a critical constraint for reliable detection of low-magnitude events in densely populated volcanic areas.

It is therefore worthwhile to propose reference noise curves specifically representative of the Campi Flegrei area, particularly considering that, due to its dense urbanization, the observed noise levels frequently exceed the reference curves defined by Peterson (1993).

Figure 10 (left) shows the normalized probability density functions (PDFs) computed from the vertical component of all the stations considered in this study, while the right panel presents the upper and lower bounds of the ambient seismic noise model derived for the Campi Flegrei caldera (see Table S1 in the Supplementary Material). These bounds are defined by the 5th and 95th percentiles of the PDF distributions and are compared with the global reference noise models NLNM and NHNM.

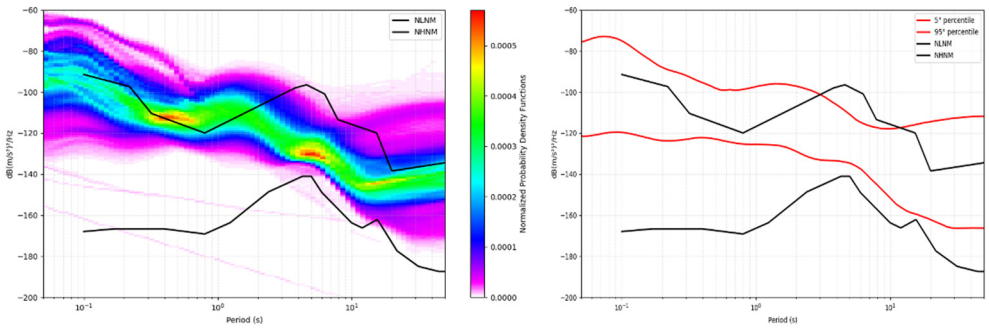

 doi:10.20944/preprints202605.0239.v1

Figure 10. (Left) Normalized PSD probability density functions for the analyzed stations in the Campi Flegrei area. (Right) Corresponding percentile envelope (5th–95th) defining the local ambient noise range, compared with the Peterson (1993) NLNM and NHNM reference models.

From an observational perspective, the analysis highlights that station performance cannot be evaluated solely through comparison with global reference models such as the Peterson NLNM and NHNM. While these models provide a useful benchmark, several stations systematically deviate from them due to site-specific conditions. In particular, stations installed in urbanized areas or close to infrastructure exhibit persistently elevated noise levels at short periods (<0.3 s), directly impacting the detectability of local volcano-tectonic signals. Conversely, underground or well-shielded installations show a significant reduction in high-frequency noise, although they may still be affected by localized sources such as railway traffic, as observed at the COLB station.

The results also indicate that natural processes play a key role in shaping the seismic noise field. Stations located near fumarolic areas display enhanced high-frequency noise, likely associated with hydrothermal fluid circulation and degassing processes [29]. This contribution is persistent over time and differs fundamentally from anthropogenic noise, suggesting that PSD analysis may provide indirect constraints on shallow hydrothermal dynamics. At intermediate periods (1–10 s), the observed shift and amplification of the secondary microseismic peak reflect the combined influence of coastal proximity and seasonal variability, while at longer periods (>10 s) the noise field becomes more spatially homogeneous, indicating dominance of regional and deep structural controls. In addition, atmospheric pressure variations may contribute to the observed noise, acting as a diffuse and persistent source even in the absence of strong local pressure gradients [30].

These findings have important implications for volcanic monitoring. Elevated and variable noise levels can significantly bias event detection, phase picking [2], and magnitude estimation, particularly during periods of low seismic energy release. Therefore, continuous PPSD monitoring should be considered an integral component of operational surveillance, supporting both real-time data quality assessment and long-term network optimization. Furthermore, understanding the frequency-dependent noise characteristics of each station provides a framework for tuning detection thresholds, optimizing filtering strategies, and guiding future station deployments in complex volcanic environments such as Campi Flegrei.

5. Conclusions

This study provides a detailed probabilistic characterization of ambient seismic noise within the Campi Flegrei caldera, highlighting the strong frequency-dependent and spatial variability of background seismic conditions in a densely urbanized volcanic environment. The results demonstrate that short-period noise systematically exceeds global reference levels at several stations, implying spatially variable detection capability and potential heterogeneity in catalog completeness across the network. The definition of a local percentile-based noise envelope represents a practical tool for realistic station performance assessment, offering a reference framework better suited to urban volcanic settings than global noise models alone. The observed reductions in noise amplitude at underground installations confirm the effectiveness of depth shielding in mitigating anthropogenic disturbances, providing objective criteria for future network optimization and station deployment strategies.

Overall, this work emphasizes that ambient seismic noise analysis is not only a diagnostic tool for network performance, but also a valuable source of information on environmental and volcanic processes. Integrating systematic PSD monitoring into routine operations can enhance the reliability of seismic observations, support the detection of weak signals, and contribute to a more robust interpretation of volcanic unrest.

 doi:10.20944/preprints202605.0239.v1

References

1. M. La Rocca e D. Galluzzo, «Seismic Monitoring of Campi Flegrei and Vesuvius by Stand-Alone Instruments,» *Ann. Geophys.*, vol. 58, n. 5, p. S0544, 2015.
2. P. Ricciolino, D. Lo Bascio e R. Esposito, *GOSSIP - Database Sismologico Pubblico INGV-Osservatorio Vesuviano*, Istituto Nazionale di Geofisica e Vulcanologia (INGV), 2024.
3. D. E. McNamara e R. P. Buland, «Ambient noise levels in the continental United States,» *Bulletin of the Seismological Society of America*, vol. 94, n. 4, pp. 1517-1527, 2004.
4. D. E. McNamara e R. I. Boaz, «Visualization of the seismic ambient noise spectrum. Seismic ambient noise,» in *Seismic Ambient Noise*, Cambridge University Press., 2019, pp. 1-29.
5. S. Bonnefoy-Claudet, F. Cotton e P. Y. Bard, «The nature of noise wavefield and its applications for site effects studies: A literature review,» *Earth-Science Reviews*, vol. 79, n. 3-4, pp. 205-227, 2006.
6. J. Groos e J. R. R. Ritter, «Time domain classification and quantification of seismic noise in an urban environment,» *Geophysical Journal International*, vol. 179, n. 2, pp. 1213-1231, 2009.
7. A. D'Alessandro, L. Greco, S. Scudero e V. Lauciani, «Spectral characterization and spatiotemporal variability of the background seismic noise in Italy,» *Earth Space Sci.*, vol. 8, n. 10, pp. 1-26, 2021.
8. J. R. Peterson, «Observations and modeling of seismic background noise,» U.S. Geological Survey, 1993.
9. INGV, *Rete Sismica Nazionale (RSN)[Data set]*, Istituto Nazionale Geofisica e Vulcanologia (INGV), 2005.
10. D. Galluzzo, L. Nardone, G. Gaudiosi, P. Cusano e A. Carandente, *INGV temporary seismic network of Osservatorio Vesuviano [Data set]*, Istituto Nazionale di Geofisica e Vulcanologia (INGV), 2024.
11. M. Vassallo, A. Bobbio e G. Iannaccone, «A Comparison of Sea-Floor and On-Land Seismic Ambient Noise in the Campi Flegrei Caldera, Southern Italy,» *Bulletin of the Seismological Society of America*, vol. 98, n. 6, p. 2962–2974, 2008.
12. Y. Gao, A. Rietbrock, F. Tilmann e E. Dushi, «High-Resolution Spatiotemporal Monitoring of Secondary Microseisms via Multi-Array Analysis,» *Geophysical Journal International*, vol. 244, n. 3, p. ggag006, 2026.
13. E. Del Pezzo, F. Bianco, M. Castellano, P. Cusano, D. Galluzzo, M. La Rocca e S. Petrosino, «Detection of seismic signals from background noise in the area of Campi Flegrei: limits of the present seismic monitoring,» *Seismol. Res. Lett.*, vol. 84, n. 2, pp. 190-198, 2013.
14. R. E. Anthony e A. T. e. a. Ringler, «How Processing Methodologies Can Distort and Bias Power Spectral Density Estimates of Seismic Background Noise,» *Seismological Research Letters*, vol. 91, n. 3, p. 1694–1706, 2020.
15. P. Welch, «The use of fast Fourier transform for the estimation of power spectra: A method based on time averaging over short, modified periodograms,» *IEEE Transactions on Audio and Electroacoustics*, vol. 15, n. 2, pp. 70-73, 1967.
16. R. E. Anthony, A. T. Ringler e D. C. Wilson, «Seismic Background Noise Levels across the Continental United States from USArray Transportable Array: The Influence of Geology and Geography,» *Bulletin of the Seismological Society of America*, vol. 112, n. 2, pp. 646-668, 2022.
17. K. G. Sabra, P. Gerstoft, P. Roux, W. A. Kuperman e M. C. Fehler, «Surface wave tomography from microseisms in Southern California,» *Geophysical Research Letters*, vol. 32, p. L14311, 2005.
18. D. H. Sheen, J. S. Shin e T. S. Kang, «Seismic noise level variations in South Korea,» *Geosci. J.*, vol. 13, pp. 183-190, 2009.
19. M. Cocco, F. Ardizzoni, R. M. Azzara, L. Dall'Olio, A. Delladio, M. D. Bona, L. Malagnini, L. Margheriti e A. Nardi, «Broadband waveforms and site effects at a borehole seismometer in the Po alluvial basin (Italy),» *Annals of Geophysics*, vol. 44, n. 1, pp. 137-154, 2001.
20. Y. Sohn, K.-H. Kim, T.-S. Kang, B. S. Ahn, D. Heo e H. Jeon, «Spatiotemporal Variation in Ambient Seismic Noise and Its Effect on the Microearthquake Monitoring Capability of the Pohang Community Seismograph Network (PCSN), South Korea,» *Bulletin of the Seismological Society of America*, vol. 116, n. 1, pp. 397-414, 2026.
21. P. Bormann e E. Wielandt, «Seismic Signals and Noise,» in *New Manual of Seismological Observatory Practice 2 (NMSOP2)*, Potsdam, Deutsches GeoForschungsZentrum GFZ: , 2013.

 doi:10.20944/preprints202605.0239.v1

22. C. Martino, L. Nardone, M. Orazi, F. Liguoro, A. Tramelli e V. Convertito, «A focused analysis on the unprecedented Peak Ground Acceleration (PGA) recorded in Italy during the 13 March 2025 Campi Flegrei Earthquake: the CSOB Case.,» 2025.
23. L. Nardone, R. S. Morelli, G. Gaudiosi, F. Liguoro, D. Galluzzo e M. Orazi, «First Steps Towards Site Characterization Activities at the CSTH Broad-Band Station of the Campi Flegrei's Seismic Monitoring Network (Italy).,» *Sensors,* vol. 25, n. 15, p. 4787, 2025.
24. S. Petrosino, N. Damiano, P. Cusano, M. A. Di Vito, S. de Vita e E. Del Pezzo, «Subsurface structure of the Solfatara volcano (Campi Flegrei caldera, Italy) as deduced from joint seismic-noise array, volcanological and morphostructural analysis,» *Geochem. Geophys. Geosyst.,* vol. 13, n. 7, 2012.
25. M. Wathelet, D. Jongmans, M. Ohrnberger e S. Bonnefoy-Claudet , «Array performances for ambient vibrations on a shallow structure and consequences over V s inversion,» *J Seismol,* vol. 12, pp. 1-19, 2008.
26. M. Picozzi, S. Parolai, D. Bindi e A. Strollo, «Characterization of shallow geology by high-frequency seismic noise tomography,» *Geophysical Journal International,* vol. 176, n. 1, pp. 164-174, 2009.
27. L. Nardone, R. Esposito , D. Galluzzo, S. Petrosino, P. Cusano, M. La Rocca, M. A. Di Vito e F. Bianco, «Array and spectral ratio techniques applied to seismic noise to investigate the Campi Flegrei (Italy) subsoil structure at different scales,» *Adv. Geosci.,* vol. 52, pp. 75-85, 2020.
28. T. Lecocq e e. al., «Global quieting of high-frequency seismic noise due to COVID-19 pandemic lockdown measures,» *Science,* vol. 369, n. 6509, pp. 1338-1343, 2020.
29. R. S. Morelli, D. Delle Donne e et al., «Seismo-Acoustic Evidence for Meteoric Water Modulation of Hydrothermal fluid discharge,» *ESS Open Archive,* 2025.
30. G. G. Sorrells, J. A. McDonald, Z. A. Der e E. Herrin, «Earth Motion Caused by Local Atmospheric Pressure Changes,» *Geophysical Journal International,* vol. 26, n. 1-4, pp. 83-98, 1971.